

## New mixed palladium—lead and palladium—tin tellurides of the NiAs type

E. Yu. Zakharova,<sup>a</sup> A. A. Isaeva,<sup>b</sup> A. N. Kuznetsov,<sup>a\*</sup> and A. V. Olenov<sup>c</sup>

<sup>a</sup>Department of Chemistry, M. V. Lomonosov Moscow State University,  
Build. 3, 1 Leninskie Gory, 119991 Moscow, Russian Federation.

Fax: +7 (495) 939 0998. E-mail: alexei@inorg.chem.msu.ru

<sup>b</sup>N. S. Kurnakov Institute of General and Inorganic Chemistry, Russian Academy of Sciences,  
31 Leninsky prosp., 119991 Moscow, Russian Federation

<sup>c</sup>Sine Theta Ltd., Scientific Park of Moscow State University,  
Build. 77, Leninskie Gory, 119992 Moscow, Russian Federation

New ternary mixed nickel arsenide-type palladium and platinum—Group 14 metal tellurides were searched for by the high-temperature ampoule synthesis combined with the X-ray powder diffraction analysis. As a result, new phases of the ternary Pd—Pb—Te and Pd—Sn—Te systems belonging to the NiAs structure type were synthesized. The crystal structure of the compound  $\text{PdPb}_{0.304(5)}\text{Te}_{0.695(5)}$  was determined by the Rietveld method ( $P6_3/mmc$ ,  $a = 4.151(1)$  Å,  $c = 5.680(1)$  Å,  $Z = 2$ ,  $R_1 = 0.032$ ,  $R_p = 0.075$ ,  $wR_{\text{all}} = 0.025$ ). It was shown that no ordering exists in the occupancy of the main-group atom site by lead and tellurium. In the Pd—Sn—Te system, a phase isostructural with the above-mentioned compound was found. In the latter phase, there is also no ordering in the occupancy of the main-group atom site. According to the electron diffraction data, a superstructure derived from the NiAs type exists in a narrow range of the compositions  $\text{PdSn}_{0.3}\text{Te}_{0.7}$ — $\text{PdSn}_{0.4}\text{Te}_{0.6}$ .

**Key words:** low-dimensional phases, layered phases, palladium—main-group metal bonds, subvalent palladium tellurides.

Investigations of compounds containing heterometallic bond systems of different dimensionality are of considerable interest because they may help in revealing the characteristic features of the formation of metal—metal bonds and particular structure types. Two structure types containing infinite heterometallic bond systems palladium—main-group metal are known. One group of compounds includes quasi-two-dimensional structures (*i.e.*, structures based on two-dimensional infinite fragments) consisting of alternating heterometallic  $\text{Cu}_3\text{Au}$ -type blocks and various non-metallic fragments, for example,  $\text{Pd}_5\text{AlI}_2$  (see Ref. 1) and  $\text{Pd}_{6.52}\text{SnTe}_2$ .<sup>2</sup> Another group of compounds include structures in which palladium—main-group metal bonds form a three-dimensional framework. These compounds crystallize in the shandite structure type  $\text{Pd}_3\text{M}_2\text{Ch}_2$  ( $\text{M} = \text{Sn, Pb}$ ;  $\text{Ch} = \text{S, Se}$ )<sup>3</sup> or the parkerite structure type  $\text{Pd}_3\text{Bi}_2\text{S}_2$  and  $\text{Pd}_3\text{Bi}_2\text{Se}_2$ ,<sup>4</sup> or, alternatively, are isostructural with the mineral ulmanite ( $\text{NiSbS}$ ), *viz.*, compounds  $\text{PdMCh}$  ( $\text{M} = \text{As, Sb, Bi}$ ;  $\text{Ch} = \text{S, Se, Te}$ ).<sup>5</sup> In addition, numerous palladium compounds belong to the intermetallics  $\text{Pd}_8\text{Sb}_3$  and  $\text{Pd}_5\text{Sb}_2$  ( $\text{Pd}_{73}\text{Sn}_{14}\text{Te}_{13}$ ,<sup>6</sup>  $\text{Pd}_5\text{Ga}_{0.71}\text{Te}_{1.42}$ , *etc.*).<sup>7</sup> In the latter case, it is assumed that the main-group metal site is statistically occupied by tellurium and Group 13–14 p-block metals.

Platinum compounds with two-dimensional infinite heterometallic fragments are much more rare. For exam-

ple, let us mention block-type bismuth—platinum iodide  $\text{Bi}_{13}\text{Pt}_3\text{I}_7$ , which has no isostructural analogs.<sup>8</sup> It should be noted that a series of cage compounds, such as ulmanites  $\text{PtMCh}$  ( $\text{M} = \text{As, Sb, Bi}$ ;  $\text{Ch} = \text{S, Se, Te}$ )<sup>5</sup> and parkerites  $\text{Pt}_3\text{Pb}_2\text{Ch}_2$  ( $\text{Ch} = \text{S, Se}$ ),<sup>9</sup> are known both for platinum and palladium. Hence, it would be expected that the behavior of platinum in the formation of chalcogenides is similar to that of palladium. Unlike platinum and palladium, nickel, which is the lighter element in the subgroup, forms more diverse mixed chalcogenides with Group 14 metals containing low-dimensional both block-type<sup>10–12</sup> and layered<sup>13–15</sup> heterometallic fragments.

The aim of the present study was to find new compounds derived from the nickel arsenide structure type and containing palladium(platinum)—main-group metal bond systems related to the mixed low-dimensional nickel tellurides  $\text{Ni}_{3-x}\text{MTe}_2$  ( $x = 0–1$ ,  $\text{M} = \text{Ge, Sn, Ga}$ ) found earlier.<sup>13–15</sup> In this type of phases based on the NiAs type (or a combination of the NiAs and  $\text{CdI}_2$  types or the NiAs and  $\text{Ni}_2\text{In}$  types), the structures are distinctly separated into layers with heterometallic nickel—main-group metal bonds due to the order in the main-group atom site. These two-dimensional fragments are terminated along the crystallographic  $c$  axis by the Te atoms, which are linked together by the van der Waals bonds. In searching for analogs of the nickel phases, we studied systems with Group 14

metals because the most abundant data on the phases  $\text{Ni}_{3-x}\text{MTe}_2$  are available for  $\text{M} = \text{Ge}$  and  $\text{Sn}$ .<sup>13,14</sup>

### Results and Discussion

According to the X-ray powder diffraction data, the sample with composition  $\text{Pd}_3\text{GeTe}_2$  contained the intermetallic compound  $\text{Pd}_2\text{Ge}$  and telluride  $\text{PdTe}_2$ . After annealing, the sample with composition  $\text{Pt}_3\text{SnTe}_2$  contained a mixture of  $\text{PtTe}_2$ ,  $\text{PtSn}$ , and  $\text{Pt}_3\text{Sn}$ , and the sample with composition  $\text{Pt}_3\text{PbTe}_2$  contained a mixture of  $\text{Pt}_3\text{Pb}$ ,  $\text{PtPb}$ , and  $\text{Pt}_3\text{Te}_4$ . Based on the phase composition of the samples after annealing, it can be concluded that the equilibrium was reached in all the samples under study. Hence, the NiAs-type ternary phases are not formed in the above-mentioned systems under the experimental conditions used.

The samples studied in the  $\text{Pd-Pb-Te}$  and  $\text{Pd-Sn-Te}$  systems contain new ternary phases. The X-ray diffraction pattern of the sample with composition  $\text{Pd}_3\text{PbTe}_2$  was fully indexed in the primitive hexagonal unit cell with the parameters  $a = 4.151(1) \text{ \AA}$  and  $c = 5.680(1) \text{ \AA}$ . The absence of superstructure reflections for  $\text{Pd}_3\text{PbTe}_2$  was confirmed by electron diffraction data (Fig. 1). The single-phase state of the sample  $\text{Pd}_3\text{PbTe}_2$  was confirmed also by the absence of the phase contrast for pressed powder samples (Fig. 2). A decrease in the amount of palladium in the  $\text{Pd}_{2.5}\text{PbTe}_2$  sample leads to the formation of  $\text{PbTe}$  as an impurity, the unit cell parameters being unchanged. Thus, the  $\text{Pd}_3\text{PbTe}_2$  phase has no noticeable regions of homogeneity with respect to palladium toward a decrease in its amount. It should be noted that the composition of the formula unit of this compound determined by X-ray powder diffraction with the use of the Rietveld method (see the Experimental section) corresponds to the formula  $\text{PdPb}_{0.304(5)}\text{Te}_{0.695(5)}$  ( $\text{Pd}_3\text{Pb}_{0.912(5)}\text{Te}_{2.085(5)}$  based on the starting weighed sample), *i.e.*, it differs only slightly from the initial stoichiometric ratio  $\text{Pd} : \text{Pb} : \text{Te} = 3 : 1 : 2$ . Taking into account the absence of impurities in this sam-

ple, which was confirmed by all the methods used, we will refer to this compound as  $\text{Pd}_3\text{PbTe}_2$ . We follow the principles of the nomenclature proposed<sup>13</sup> for the first representatives of the family, *viz.*, compounds  $\text{Ni}_3\text{GeTe}_2$  and  $\text{Fe}_3\text{GeTe}_2$ , which, according to the structural data, are characterized by a deficiency of transition metals compared to the above-considered stoichiometry.

In the  $\text{Pd-Sn-Te}$  system, five compositions were investigated (Table 1, see the Experimental section). The X-ray powder diffraction patterns of the samples were also indexed in the primitive hexagonal unit cells (Table 2). Sample 4 with the initial stoichiometry « $\text{Pd}_2\text{SnTe}_2$ » contained substantial impurities of  $\text{Pd}_{1-x}\text{Te}$  and  $\text{SnTe}$ . Sample 5 with the initial stoichiometry « $\text{Pd}_3\text{Sn}_2\text{Te}$ » contained impurities of  $\text{SnTe}$ ,  $\text{Pd}_{17}\text{Te}_4$ , and  $\text{Pd}_9\text{Te}_4$ . This indicates that the actual composition of the ternary phases of the samples under consideration differs from the initial stoichiometry. In sample 1 with the ratio  $\text{Pd} : \text{Sn} : \text{Te} = 3 : 1 : 2$ , which is virtually in the single-phase state (according to the X-ray powder diffraction data), only trace amounts of palladium were detected by scanning electron microscopy (SEM) (see Fig. 2) and energy-dispersive X-ray analysis (EDX). In samples 2 and 3, no impurity phases were found by X-ray powder diffraction and EDX.

Studies of samples 2 and 3 by the electron diffraction method (Fig. 3) confirmed that the samples « $\text{Pd}_{2.6}\text{SnTe}_2$ » and « $\text{Pd}_3\text{Sn}_{0.6}\text{Te}_{2.4}$ » contain only the NiAs-type phase with the unit cell parameters corresponding to those determined by the indexing of the X-ray powder diffraction patterns (see Table 2). Hereinafter, we will refer to the latter phase as disordered (because the main-group metal site in ternary phases with the NiAs-type unit cell is necessarily statistically occupied by different elements). For the chosen crystals of compositions  $3 : 1 : 2$ ,  $3 : 2 : 1$ , and  $2 : 1 : 2$ , a superstructure with respect to the NiAs-type unit cell was observed. This superstructure is not analogous to that found earlier for  $\text{Ni}_{3-x}\text{MTe}_2$ -type phases and requires further investigation. It should be noted that there is a correlation between the unit cell parameter  $c$  for the phases without

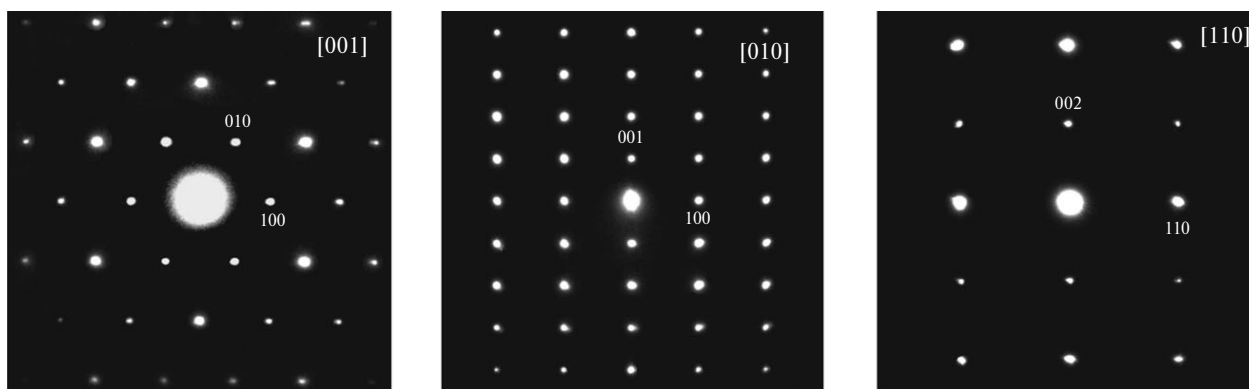
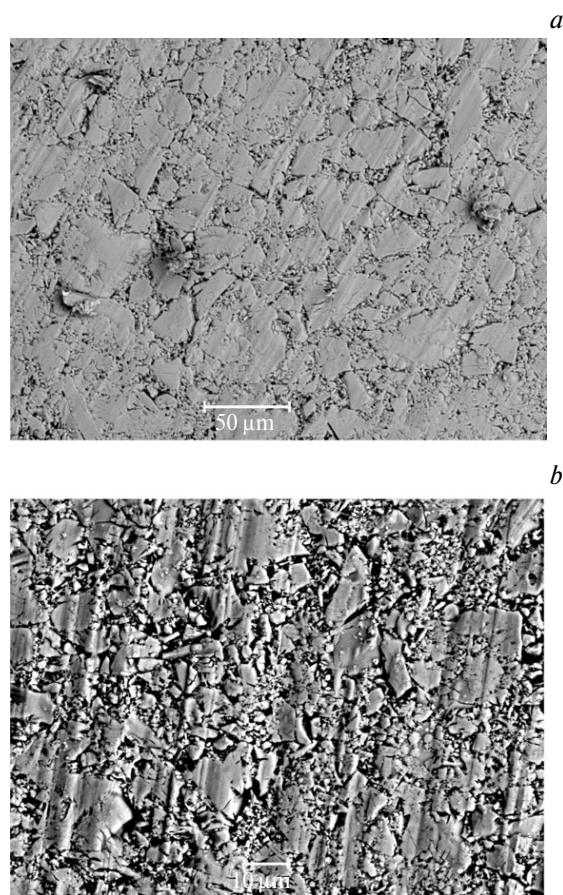


Fig. 1. Main zone diffraction patterns for the sample with composition  $\text{Pd}_3\text{PbTe}_2$ .



**Fig. 2.** SEM photomicrographs of pressed samples with the starting compositions  $\text{Pd}_3\text{PbTe}_2$  (a) and  $\text{Pd}_3\text{SnTe}_2$  (b).

a superstructure and the phases with a superstructure with respect to NiAs. Thus, the indexing without consideration for the superstructure resulted in the unit cell parameter  $c$  in the range of 5.61–5.64 Å for phases with the disordered NiAs-type structures and in the range of 5.53–5.55 Å for phases with the NiAs-type superstructure. According

**Table 1.** Nominal compositions and the annealing times ( $\tau$ ) at 750 °C of samples in the Pd–M–Te (M = Ge, Sn, Pb) and Pt–M–Te (M = Sn, Pb) systems

Sample	Nominal composition	$\tau$ /day
1	$\text{Pd}_3\text{SnTe}_2$	1) 14; 2) 5
2	$\text{Pd}_3\text{Sn}_{0.6}\text{Te}_{2.4}$	8
3	$\text{Pd}_{2.6}\text{SnTe}_2$	8
4	$\text{Pd}_2\text{SnTe}_2$	1) 8; 2) 4
5	$\text{Pd}_3\text{Sn}_2\text{Te}$	1) 8; 2) 4
6	$\text{Pd}_3\text{PbTe}_2$	8
7	$\text{Pd}_{2.5}\text{PbTe}_2$	1) 6; 2) 5
8	$\text{Pd}_3\text{GeTe}_2$	8
9	$\text{Pt}_3\text{SnTe}_2$	17
10	$\text{Pt}_3\text{PbTe}_2$	11

**Table 2.** Crystallographic data for samples 1–5

Sample	$a$	$c$
	Å	
1	4.0806(9)	5.551(1)
2	4.1222(6)	5.6419(6)
3	4.0969(5)	5.6123(5)
4	4.0728(7)	5.5315(7)
5	4.0648(6)	5.552(1)

to the EDX data, the compositions of all crystals, for which the superstructure was observed, are in the range  $\text{Pd}_3\text{Sn}_{0.9}\text{Te}_{2.1}$ – $\text{Pd}_3\text{Sn}_{1.2}\text{Te}_{1.8}$ . Crystals with this composition featuring an ordering were found in the samples with the ratio of the elements equal to 3 : 1 : 2 and 2 : 1 : 2, as well as to 3 : 2 : 1. For sample 1, these crystals were the only product, whereas the amount of such crystals in samples 4 and 5 was very low. Taking into account that the latter two samples were not single-phase (according to the X-ray powder diffraction data), the formation of an ordered phase in these samples can be considered as a local effect. Apparently, the region of the existence of the phase with additional ordering is narrow, and a compound with the disordered NiAs-type structure is the major compound in this system. Here, the main-group atom site is statistically occupied by tin and tellurium. The absence of detectable impurities in samples 2 and 3 indicates that the phase is not a pointwise phase and can have a region of homogeneity with respect to palladium (like mixed nickel–tin tellurides) and that the ratio of the elements in the main-group atom site deviates from Sn : Te = 1 : 2 toward an increase in the amount of tellurium. Since tin and tellurium are virtually indistinguishable by X-ray diffraction methods due to the similarity of their atomic scattering factors, we did not pursue the X-ray structure study in this case.

The crystal structure of  $\text{Pd}_3\text{PbTe}_2$  determined by the Rietveld refinement is shown in Fig. 4, a. Figure 4, b presents the structure of  $\text{Ni}_3\text{GeTe}_2$  for comparison. Figures 4, c, d show the projections of the corresponding structures onto the  $ab$  plane. The Pd–(Pb/Te) distances are 2.786(1) Å. The Pd–Pd and (Pb/Te)–(Pb/Te) distances are non-bonding (4.151(1) and 3.716(1) Å, respectively).

Figure 5 illustrates the structural transition between the disordered sample  $\text{Pd}_3\text{PbTe}_2$  and two layered phases  $\text{Ni}_{3-x}\text{MTe}_2$  limiting with respect to the nickel content, viz.,  $\text{Ni}_3\text{MTe}_2$  and  $\text{Ni}_2\text{MTe}_2$ .

Thus, there is no superstructure ordering of tellurium and p-block metal atoms in the As site in NiAs-type palladium–p-block metal tellurides synthesized in the present study compared to the layered  $\text{Ni}_{3-x}\text{MTe}_2$ -type nickel tellurides. This is why the NiAs-type based unit cell for pal-

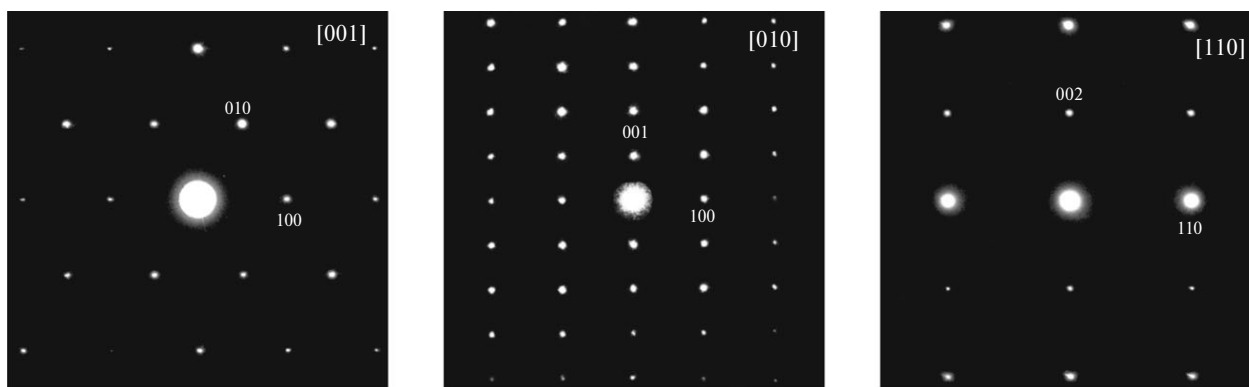


Fig. 3. Main zone diffraction patterns for the sample with the starting composition  $\text{Pd}_3\text{Sn}_{0.6}\text{Te}_{2.4}$ .

ladium compounds is not increased by a factor of three, as opposed to nickel phases. Consequently, unlike  $\text{Ni}_{3-x}\text{MTe}_2$ -type phases, both the van der Waals gap be-

tween two successive series of tellurium atoms and pronounced  $\text{Ni}_2\text{In}$ -type heterometallic layers also derived from the  $\text{NiAs}$  structure type are absent in the compounds

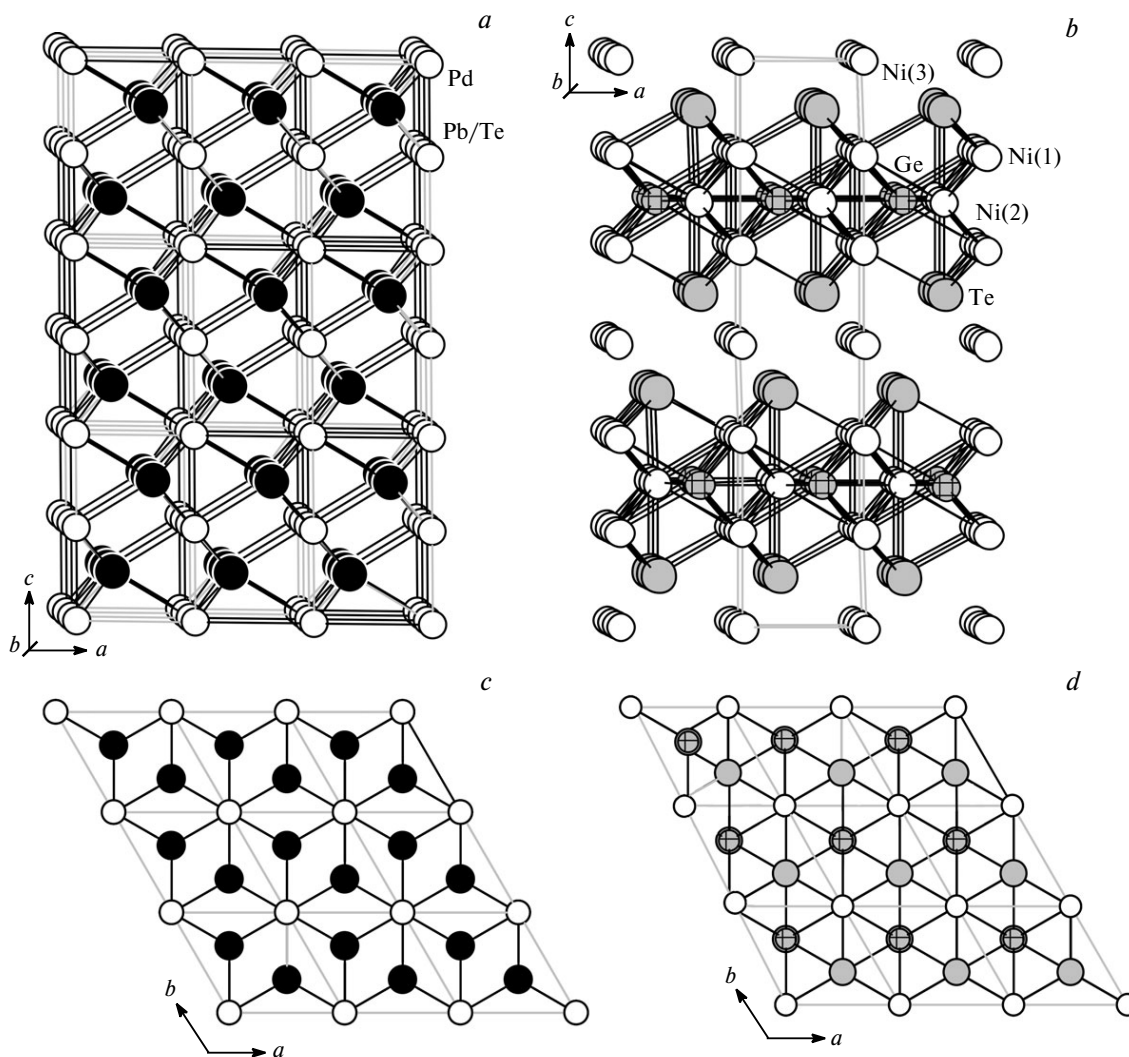
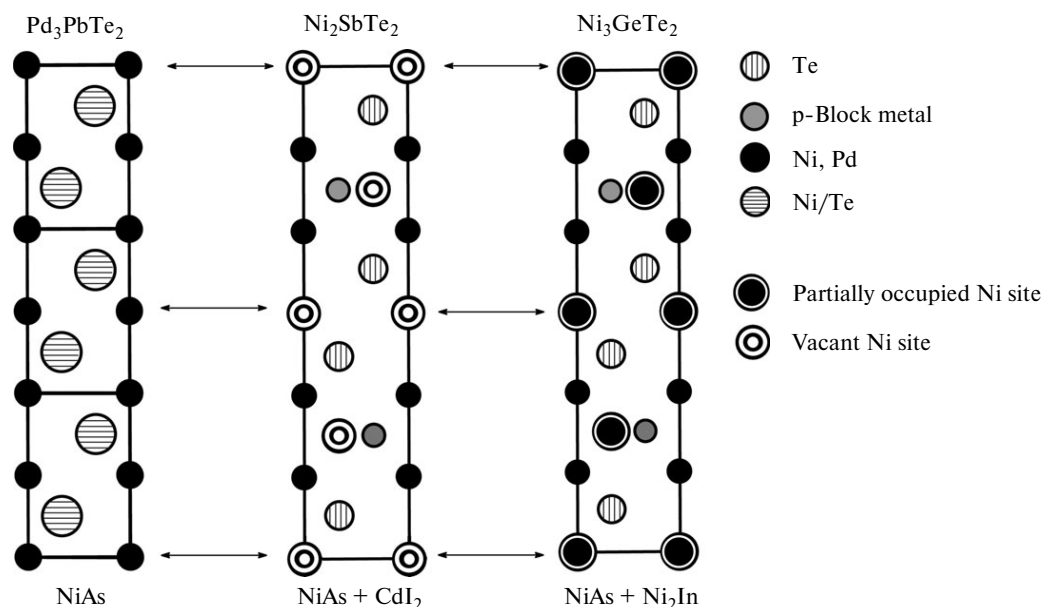


Fig. 4. Crystal structures of  $\text{Pd}_3\text{PbTe}_2$  (a, c) and  $\text{Ni}_3\text{GeTe}_2$  (b, d).



**Fig. 5.** Transition between the disordered structure  $\text{Pd}_3\text{PbTe}_2$  and the ordered mixed nickel—p-block metal tellurides derived from the NiAs structure type.

under consideration (see Fig. 5). The exception is the region of the compositions  $\text{Pd}_3\text{Sn}_{0.9}\text{Te}_{2.1}$ — $\text{Pd}_3\text{Sn}_{1.2}\text{Te}_{1.8}$  in the Pd—Sn—Te system, where, apparently, a superstructure is formed. The latter was observed by the electron diffraction method. Experiments on the determination of the structure of the phase in this regions are underway. Nevertheless, the available data show that this phase is not the direct analog of  $\text{Ni}_{3-x}\text{MTe}_2$ -type phases.

It should also be noted that there is the difference in the behavior of the compounds in the Pd—Sn—Te and Pd—Pb—Te systems with respect to a decrease in the palladium content in the unit cell. Phases of the  $\text{Ni}_{3-x}\text{MTe}_2$  family are characterized by the parameter  $x$ , which varies in a rather wide range (from 0—0.2 to 1). A similar situation is observed for palladium—tin tellurides. Thus, a decrease in the amount of palladium in the samples leads to a change in the parameters of the hexagonal unit cell (although the EDX and X-ray powder diffraction data indicate that the lower limit of the palladium content in the sample is substantially higher compared to the nickel phases). This is not observed in the Pd—Pb—Te system. Thus, a decrease in the percentage of palladium in the samples results in the appearance of impurities, whereas the unit cell parameters of the hexagonal phase remain unchanged. Factors responsible for the difference in the behavior of lead and tin systems remain unclear. However, it is the difference in the radius of main-group metals that makes the formation of palladium vacancies near lead atoms unfavorable and plays apparently the main role. It should be noted that the factors responsible for the presence or absence of the additional ordering in compounds based on the NiAs and  $\text{Ni}_2\text{In}$  structure types remain unknown. Even

in the dedicated reviews on the superstructures based on these structure types,<sup>16</sup> the authors mostly limit themselves to just stating the facts.

## Experimental

Palladium (foil, 99.99%), Pt (powder, 99.99%), Pb (ingot, 99.99%), Ge (powder, 99.99%), Sn (powder, 99.99%), and Te (special purity grade) were used for the synthesis. Stoichiometric mixtures of the starting compounds were placed in quartz ampoules, which were evacuated to the residual pressure of  $\sim 5 \cdot 10^{-2}$  Torr and then sealed using an oxygen burner flame. The annealing was performed in a Nabertherm furnace in the programmed heating mode (the accuracy of the temperature measurement was  $\pm 1^\circ\text{C}$ ). The initial stoichiometry and the mode of annealing are given in Table 1. The initial algorithm of the search involved the synthesis of samples with the stoichiometry  $\text{Pd}(\text{Pt}) : \text{M} : \text{Te} = 3 : 1 : 2$  followed by the synthesis of a series of samples of different compositions in the Pd—Sn—Te synthesis with the aim of refining the region of the existence of the desired phase and the synthesis of an additional sample in the Pd—Pb—Te system for the purpose of investigating the behavior of the phase with respect to the palladium depletion. The samples were heated to  $750^\circ\text{C}$  for 8—10 h. To increase the rate of the establishment of the equilibrium between the successive annealing steps, polycrystalline cakes were thoroughly homogenized in an agate mortar.

The X-ray powder diffraction analysis of polycrystalline samples was carried out on a FR-552 Guinier—de Wolff three-frame monochromator camera (Enraf Nonius) ( $\text{Cu-K}\alpha_1$  radiation,  $\lambda = 1.54051 \text{ \AA}$ ) and a Stoe STADI-P automated powder diffractometer. The X-ray diffraction patterns were analyzed with the use of the WinXPow software package and the ICDD PDF2 database.<sup>17</sup> In studies with the use of the Guinier—de Wolff monochromator camera, a germanium powder (99.9999%) was

**Table 3.** Structure refinement statistics for Pd<sub>3</sub>PbTe<sub>2</sub>

Parameter	Value
Formula unit	PdPb <sub>0.304(5)</sub> Te <sub>0.695(5)</sub>
<i>T</i> /K	293
Space group	<i>P</i> 6 <sub>3</sub> / <i>mmc</i>
<i>a</i> /Å	4.151(1)
<i>c</i> /Å	5.680(1)
<i>V</i> /Å <sup>3</sup>	84.75(3)
<i>Z</i>	2
2θ-Scan range/deg	20 < 2θ < 119.99
Number of refined parameters	30
<i>R</i> <sub>1</sub> , <i>R</i> <sub>p</sub> , <i>wR</i> <sub>all</sub>	0.032, 0.075, 0.025
Type of the profile function	Pseudo-Voigt

used as the internal standard. The X-ray diffraction patterns were processed with an IZA comparator with an accuracy of ±0.02 mm.

The crystal structure of Pd<sub>3</sub>PbTe<sub>2</sub> was refined by the full-profile Rietveld method based on the X-ray powder diffraction data obtained on the Stoe STADI-P diffractometer (Cu-Kα<sub>1</sub> radiation, λ = 1.54051 Å, germanium monochromator). The refinement was carried out with the use of the Jana 2000 program.<sup>18</sup>

The structure refinement statistics are given in Table 3. The thermal parameters were refined isotropically. The Pb-to-Te ratio in the site 2c was refined with restraints on the total occupancy of the site (100%). The refinement was performed with the use of 31 reflections. According to the results of the refinement of the Pb-to-Te ratio, the exact formula of the new phase can be written as Pd<sub>3</sub>Pb<sub>0.912(5)</sub>Te<sub>2.085(5)</sub>, which is in good agreement (within experimental error) with the required stoichiometry 3 : 1 : 2.

The microstructure of the samples was studied with a LEO Supra 50VP high-resolution scanning electron microscope. The EDX analysis was carried out with this microscope equipped with an Oxford Instruments INCA Energy+ system for micro-analysis (the accelerating voltage was 15–25 kW, the acquisition time was 120 s, the maximum error in the determination was 2 at.%). Electron diffraction experiments were performed with a JEOL JEM-2100F high-resolution transmission electron microscope (the accelerating voltage was 200 kV).

This study was financially supported by the Russian Foundation for Basic Research (Project No. 09-03-12296) and the Presidium of the Russian Academy of Sciences (Program for Basic Research "Development of Methods

for the Synthesis of Chemical Compounds and the Design of New Materials").

## References

1. H.-B. Merker, H. Schäfer, B. Krebs, *Z. Anorg. Allg. Chem.*, 1980, **462**, 49.
2. S. V. Savilov, A. N. Kuznetsov, B. A. Popovkin, V. N. Khrustalev, P. Simon, J. Getzschmann, Th. Doert, M. Ruck, *Z. Anorg. Allg. Chem.*, 2005, **631**, 293.
3. S. Natarajan, G. V. Subba Rao, R. Baskaran, T. S. Radhakrishnan, *J. Less-Common Met.*, 1988, **138**, 215.
4. K.-J. Range, M. Zabel, S. Wandering, H. P. Bortner, *Rev. Chim. Miner.*, 1983, **20**, 698.
5. F. Hulliger, *Nature*, 1963, **198**, 761.
6. F. Laufek, A. Vymazalova, J. Plasil, *Powder Diffraction*, 2007, **22**, 334.
7. M. El-Boragy, K. Schubert, *Z. Metallkunde*, 1971, **62**, No. 4, 314.
8. M. Ruck, *Z. Anorg. Allg. Chem.*, 1997, **623**, 1535.
9. F. A. Bannister, M. H. Hey, *Mineral. Mag. Mineral. Soc.*, 1932, **23**, 188.
10. A. I. Baranov, A. A. Isaeva, L. Kloov, B. A. Popovkin, *Inorg. Chem.*, 2003, **42**, 6667.
11. A. A. Isaeva, A. I. Baranov, Th. Doert, B. A. Popovkin, V. A. Kulbachinskii, P. V. Gurin, V. G. Kytin, V. I. Shtanov, *J. Solid State Chem.*, 2007, **180**, 221.
12. A. A. Isaeva, A. I. Baranov, Th. Doert, M. Ruck, V. A. Kulbachinskii, R. A. Lunin, B. A. Popovkin, *Izv. Akad. Nauk, Ser. Khim.*, 2007, 1632 [*Russ. Chem. Bull., Int. Ed.*, 2007, **56**, 1694].
13. H.-J. Deiseroth, K. Aleksandrov, C. Reiner, L. Kienle, R. K. Kremer, *Eur. J. Inorg. Chem.*, 2006, **8**, 1561.
14. O. N. Litvinenko, A. N. Kuznetsov, A. V. Olenov, B. A. Popovkin, *Izv. Akad. Nauk, Ser. Khim.*, 2007, 1879 [*Russ. Chem. Bull., Int. Ed.*, 2007, **56**, 1945].
15. A. A. Isaeva, O. N. Makarevich, A. N. Kuznetsov, Th. Doert, A. M. Abakumov, G. van Tendeloo, *Eur. J. Inorg. Chem.*, 2010, 1395.
16. S. Lidin, A.-K. Larsson, *J. Solid State Chem.*, 1995, **118**, 313.
17. *STOE WinXPow, Version 1.06*, STOE and Cie GmbH, 1999.
18. V. Petricek, M. Dusek, L. Palatinus, *Jana2000, The Crystallographic Computing System*, Institute of Physics, Praha, Czech Republic, 2000.

Received June 24, 2010;  
in revised form January 24, 2011